RSC Advances

ROYAL SOCIETY OF CHEMISTRY

www.rsc.org/advances

Journal Name

ARTICLE

Hierarchically porous polystyrene membranes fabricated *via* CO_2-expanded liquid selectively swelling and *in situ* hyper-cross-linking method†

Received 00th January 20xx,
Accepted 00th January 20xx

DOI: 10.1039/x0xx00000x

www.rsc.org/

Haozong Wang,[a] Hua Bai,[a] and Lei Li[*ab]

Hierarchically porous polymeric materials represent a new class of materials that have attracted both industrial and academic interests. This paper presents a novel, etching-free and versatile preparation methodology, using commercially available polystyrene *via* CO_2-expanded liquids selectively swelling process combined with hyper-cross-linking reaction. The morphology of the membranes was observed with electron microscopes, and the chemical structure of the membranes was investigated by Fourier transformation infrared spectrometry and Solid-state nuclear magnetic resonance measurement. One level of macroporous structures was produced by CO_2-expanded methanol selective swelling process, while the other level of micropores was created *via* the hyper-cross-linking reaction. The cross-linked membranes showed large specific surface areas and excellent thermal stability, which have potential applications in catalysis, separation and gas storage.

Introduction

In the past decades, the preparation of hierarchically porous materials has attracted both industrial and academic interests due to their charming properties combined with the characteristic structures.[1-5] Although a mass of hierarchically porous inorganic materials have been prepared, it still keeps challenges to fabricate hierarchical porous polymeric materials.[6-11] Currently, the most widely used methodology of creating porosity in polymers is based on the micro-phase separation of block copolymers (BCPs),[12-18] thus several techniques for preparing hierarchical porous polymeric materials have been devised. For example, Russell *et al.* prepared hierarchically porous polymeric membranes with diblock copolymer polystyrene-*b*-poly(n-butyl methacrylate) (PS-*b*-PnBMA). They first constructed PS-*b*-PnBMA membranes micrometer-scale pores *via* breath figure processing, and then degraded the component of PnBMA by UV irradiation, to produce nanoscale pores. As a result, the hierarchically porous polymer membranes in micro/nano-scale were obtained.[19] In another example, Sai *et al.* put forward a method for acquiring hierarchically porous BCP-derived materials dubbed the spinodal-decomposition induced macro- and mesophase separation plus extraction by rinsing process. A BCP was first dissolved in an organic solvent with a small molecule additive, which could selectively swell one of the blocks of the BCP. Then the solvent was evaporated in a controlled manner. The dried film was then placed in a rinsing solution in order to remove the oligomeric additive. After the processes aforementioned, hierarchical and continuous porosity in the polymer matrix was generated.[8]

Although the above methods can be used to prepare hierarchical porous polymeric materials, they are confronted with several drawbacks. The synthesis parameter window of BCPs in their synthetic processes is narrow, and the phase separation process of BCPs needs careful control of the experimental conditions. Besides, additional chemical reaction is needed to decompose the specific segments of the BCPs. These disadvantages strongly limit the development of hierarchically porous polymeric materials, thus an easy and etching-free method is desired.

Recently some novel template-free strategies of creating pores in polymer matrices have been developed,[20-22] and they are inspiring us to design new strategies of preparing hierarchical porous polymeric materials. CO_2-expanded liquid (CXL) is a mixed solvent composed of compressible CO_2 dissolved in an organic solvent.[23] By increasing the CO_2 pressure, the properties of the mixed solvent change from a pure organic solvent to supercritical CO_2 ($scCO_2$). Compared with $scCO_2$, CXLs possess the ability to dissolve polar compound,[23-24] thus CXLs are applicable to construct porous structure in a variety of polymers with low affinity to $scCO_2$.[22, 25] Therefore, CO_2-expanded methanol was used in our group to

[a] College of Materials, Xiamen University, Xiamen 361005, People's Republic of China. E-mail: lilei@xmu.edu.cn; Tel: +86-592-2186296; Fax: +86-592-2183937.
[b]. State Key Laboratory for Modification of Chemical Fibers and Polymer Materials, Donghua University, Shanghai 201620, People's Republic of China
† Electronic Supplementary Information (ESI) available. See DOI: 10.1039/x0xx00000x

construct nanostructures in an amphiphilic BCP of PS-*b*-PVP.[22] Though neither polystyrene (PS) nor poly(vinylpyridine) (PVP) has high affinity to CO_2, while methanol is a good solvent to PVP segments. Thus, CO_2-expanded methanol could plasticize PS matrix and selectively swell PVP component simultaneously, inducing the phase transition and generating nano-network. After isobar quenching and depressurization, porous structures were formed in the polymer matrix. Another commonly used method to introduce micropores into polymer films and monoliths is hyper-cross-linking reaction, which is most frequently performed by Friedel-Crafts alkylation.[26] The hyper-cross-linking reaction produces cross-linking bonds between polymer chains, leaving molecular-sized pores between them. Therefore, the hyper-cross-linked polymers exhibit attractive properties such as ultra-high surface area and the excellent adsorbing ability.[26-32]

Herein we report a new strategy to prepare hierarchically porous membranes with commercial available PS, combining CO_2-expanded methanol processing with a sequent hyper-cross-linking post-treatment. One level of the pores was first generated by CO_2-expanded liquid processing, and the other level was produced by the sequent Friedel-Crafts hyper-cross-linking reaction. Compared with the above-mentioned methods involving BCP templates, our strategy has the following advantages: firstly, commercial available polymer instead of BCPs is used, thus no complex synthesis is needed; secondly, phase separation process is unnecessary in this method; last, no etching processing is required to generate porosities. Thus this strategy provides a novel, etching-free and versatile way to prepare hierarchically porous polymeric membranes.

Materials and methods

Materials

A commercially available PS sample with a molecular weight (*Mw*) of 214.8 k and a polydispersity index (PDI) of 1.67, was purchased from Asahi Chemical Company. Dimethoxymethane (FDA) was bought from Tokyo Chemical Industry Co., Ltd, and iron (III) chloride (98%) was the product of Alfa Aesar Company and used without further purification. Toluene, Tween-85 and 1,2-dichloroethane (DCE) (analytical pure) was purchased from Sinopharm Chemical Reagent Co., Ltd. DCE was washed with concentrated H_2SO_4, aqueous Na_2CO_3 and water for several times, then refluxed with CaH_2 and fractionally redistilled. Methanol (chromatographically pure) was bought from J&K Chemical. CO_2 with 99.99% purity was supplied by Xinhang Gas (Fuzhou, China). All the chemical reagents were used as received without further purification unless specifically noted.

Preparation of nonporous polystyrene membranes

PS solution was prepared by stirring PS pellets in toluene at room temperature. A certain amount of non-ionic surfactant Tween-85 was then added into the PS solution, and the mixture was stirred at least 30 min to obtain a homogeneous solution. The solution was cast onto a clean glass substrate. After the evaporation of the solvent, a transparent membrane was formed. The membrane was further dried in vacuum for 24 h.

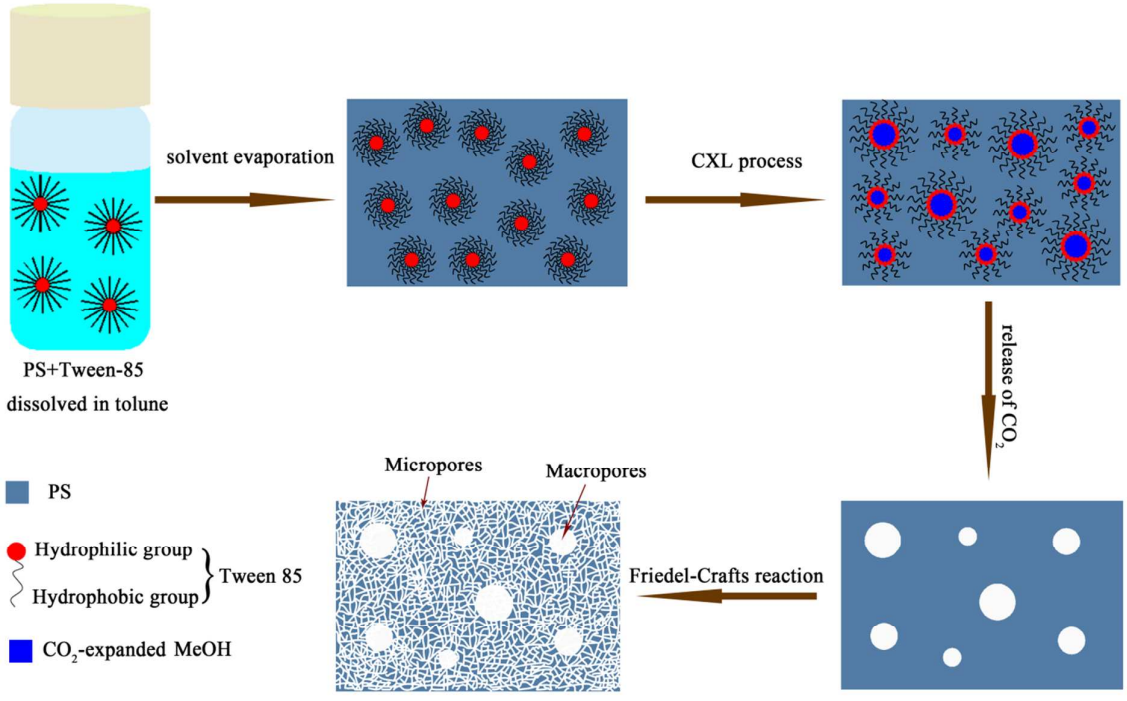

Scheme 1 Illustration of the preparation of hierarchically porous PS membrane.

The dry membrane was cut into small pieces (10 × 30 mm) and transferred into a high-pressure vessel containing 1 mL methanol. CO_2 was added using a high performance liquid chromatography pump (Jasco PU-2086 plus, Japan) to expand methanol and swell the membrane. A back-pressure regulator (Jasco BP-2080 plus, Japan) was used to control the vessel pressure in a dynamic balance. The temperature of the vessel was controlled by a thermostatic water bath (±0.5 °C) (Jinghong DK-S22, Shanghai, China). The processing time for each sample was 30 min. Before releasing the CO_2, the vessel was quenched by transferring into an ice bath. The release of CO_2 was controlled by the back-pressure regulator with a speed of 0.5 MPa min^{-1}.

Hierarchically porous polymeric membranes *via* hyper-cross-linking

$FeCl_3$ (1.625 g, 0.005 mol), FDA (0.38 g, 0.005 mol) and 5 mL DCE were combined and stirred in a flask until completely mixed. Several pieces of PS macroporous membranes after CXL process were added to the mixture, and then the mixture was heated and kept at 80 °C for 8 h without stirring to hyper-cross-link the membranes. The resulted membranes were collected and washed with methanol for three times, extracted with Soxhlet extractor for 12 h, and finally dried under vacuum at 60 °C for 24 h.

Characterization

The morphology of honeycomb membranes was observed by scanning electron microscopy (SEM) (SU-70, Hitachi) under an electron beam with an accelerating voltage of 10 kV and a working distance of 15 mm. For the cross-section observation, the membrane was frozen and fractured in liquid nitrogen. All the samples were coated with a thin layer of gold before observation. The hierarchically porous structures of the membranes were characterized by high-resolution transmission electron microscopy (TEM) (JEM-2100) with an acceleration voltage of 200 kV. Thermal Gravity Analysis (TGA) of the cross-linked membranes was performed on a thermal analyzer (Q500 V6.7 Build 203) under air atmosphere with a heating rate of 10 °C min^{-1}. Specific surface areas of the membranes were measured on a surface and porosity analyzer (TRISTAR II3020). Fourier transform infrared spectra (FT-IR) were obtained with a NICOLET iS10 spectrometer. Solid-state nuclear magnetic resonance (NMR) spectra was collected on a BRUKER AV 400 spectrometer.

Results and discussion

The preparation of hierarchically porous PS membranes is schematically shown in Scheme 1. A PS/Tween-85 blend membrane was obtained by casting the corresponding solution, and then transferred into high-pressure vessel containing methanol inside in order to carry out CXL process, during which macropores were generated in the PS matrix. The macroporous PS membranes were then hyper-cross-linked in DCE by FDA, to produce micropores. Eventually, a hierarchically porous PS membrane was obtained.

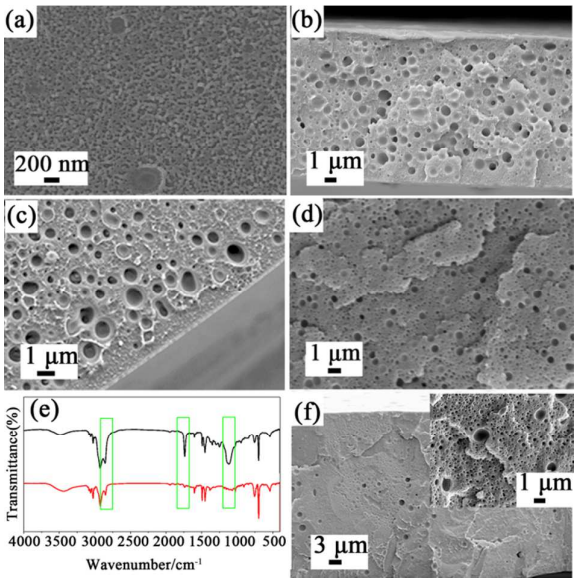

Fig 1 (a) Cross-sectional SEM image of blend membrane after methanol extraction. (b-d) Cross-sectional SEM images of blend membrane processed after CO_2-expanded methanol processing (b-global view, c-edge of membrane, d-center of membrane). (e) FT-IR spectra of the raw PS membrane (black curve) and PS membrane after CXL treatment (red curve). (f) Cross-sectional view of blend membrane after 3 minute CXL treatment (Inset: a magnified cross-section view).

Firstly, the distribution of Tween in the PS membrane was examined. The as-prepared PS/Tween-85 blend membrane was fractured in liquid nitrogen and the fracture surface was extracted by methanol for 24 h. After drying, the cross-section was observed by SEM and shown in Fig 1a. The image evidently demonstrates that the uniform and dense pores with the diameter of 26 ± 8 nm and a density of 1.16×10^{15} cells/cm^3 is formed. The porosity is ascribed that the Tween-85 embedded inside the film is washed out of the fractured surface after extraction, indicative of a uniform distribution of Tween-85 in PS matrix.[33] In addition, because of the amphiphilicity of Tween-85, it is reasonable to believe that Tween-85 form micelles in the PS matrix, with hydrophobic groups toward PS matrix.

The PS/Tween-85 blend membrane (containing 3 wt% Tween-85) was then treated by CO_2-expanded methanol at 45 °C and 10 MPa for 30 min, following the procedures mentioned in the Experimental Section, to produce macroporous. After the CXL process, the macrostructure in the film were confirmed with SEM, as shown in Fig 1b. Usually, the conventional $scCO_2$ foaming process always results in a dense unfoamed skin as thick as dozens of micrometers. In our case, the surface skin is less than 2 μm, which is similar to that produced by a surface constrained foam process.[34] The characteristic thin surface skin and macrostructures are attributed to that the surfactants near the membrane surface diffuse from the matrix into the liquid phase prior to the foaming step, while the surfactants inside the film worked as porogen, as discussed below.

It is found that the T_g of the matrix polymer significantly influences the rearrangement time, which can be reduced from

30 min to 10 seconds when the T_g decreased from 95 °C to -69 °C.[35-36] The saturation temperature of 45 °C is well above the T_g of PS in CO_2 under 10 MPa pressure.[37] Therefore, upon charging of the vessel with CO_2, PS matrix is significantly plasticized. Additionally, the effective interaction between PS and additives can also be significantly reduced. Thus, the CO_2-methanol can penetrate into the bulk material through the film and selectively swells the Tween-85 micelles beneath the top PS layer. In the following isobar quenching, the PS matrix is frozen and the trapped CO_2 droplets are fixed in the PS matrix. Therefore, macro cellular structures are obtained after depressurization.[38] In Fig 1d, macropores with an average diameter of 500 ± 280 nm and density of 1.30×10^{12} cells/cm^3 are observed (The histogram of pore sizes distribution after CXL process calculated according to the SEM image is shown in Figure S1 a). The increasing of pore size and decreasing of aggregation number (number density), compared with that in the membrane after methanol extraction indicates the rapid structural reconstruction during the CXL process.

The comparison of the FT-IR spectra of the films before and after CXL treatment is plotted in Fig 1e. It is found that the intensity of the bands associated with C-O-C groups, ester groups and C=C groups of Tween-85 at 1109 cm^{-1}, 1757 cm^{-1} and 2856 cm^{-1} become much weaker after CXL processing, indicating that most Tween-85 is removed from the PS matrix during CXL processing. Furthermore, a contrast experiment was completed after 3 min CXL treatment. The similar porous morphology is observed in the cryo-fractured cross-section, as shown in Fig 1f. It should be note that the pore size (162 ± 86 nm) is smaller and uniform and the number density (8.7×10^{15} cells/cm^3) is higher compared with that in the film after 30 min CXL treatment as shown in Fig1f, while the thickness of surface skin keeps unchanged. Therefore, we can conclude that the Tween-85 molecules close to the surface is washed out at the beginning of CXL treatment, while the Tween-85 micelles in the middle of the film firstly trap the CO_2 droplets and then gradually merge. With the elongation of processing time, the Tween-85 molecules inside the film are also extracted by the methanol through the swollen PS matrix. The trapped CO_2 droplets keep intact because of the isotropic chemical potential inside the high-pressure vessel until the morphology is fixed by isobar quenching. The detailed investigation of the influence of the ratio of Tween-85 to PS, experiment conditions and species of surfactant on the morphology of the porous membrane will be described elsewhere.

The N_2 adsorption isotherm of the blend membrane after CXL processing was measured at liquid nitrogen temperature and is shown in Fig 2. The membranes were frozen by liquid nitrogen and fractured into small pieces before the experiment in order to expose the pores. However, a rather low BET specific surface area of 1.73 m^2 g^{-1} was obtained, although the membranes are highly porous. Such low specific surface area reveals that the CXL membrane has a close-pore structure.[39]

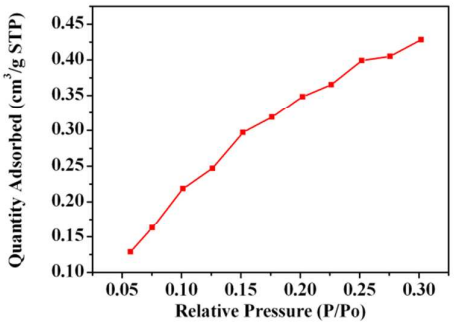

Fig 2 N_2 adsorption isotherm of the blend membrane after CO_2-expanded methanol treatment.

In order to produce additional micropores in the porous PS membrane, a hyper-cross-linking reaction was performed. The cross-linking process of PS membranes was realized by soaking the membranes in the mixture of $FeCl_3$, FDA and DCE at 80 °C for 8 h. After cross-linking reaction the hyper-cross-linked membranes were washed with methanol for several times and then Soxhlet extracted with methanol overnight followed by drying in vacuum for 12 h. The hyper-cross-linking mechanism has been investigated by several researchers.[40-46] During the cross-linking process, FDA was acted as an external cross-linker to connect the benzene rings on PS backbones, through Friedel-Crafts reaction. To confirm the chemical structure of the hierarchically porous PS membrane, FT-IR spectra of the PS membrane before and after hyper-cross-linking reaction were reported, as shown in Fig 3. In the spectrum of the cross-linked membrane, a new band appears at 817 cm^{-1}, which is assigned to multi-substituted benzene ring and in line with the data reported by Law *et al.*[43] The intensity of the band associated with mono-substituted benzene ring at 710 cm^{-1} becomes weaker compared with that of uncross-linked membrane. These data demonstrate that the hydrogens on benzene ring were substituted in the reaction. The intensity of the bands at 3059 and 3080 cm^{-1}, which is associated with the hydrogens on the aromatic rings, are obviously reduced, also verifying the substitute reaction on the benzene rings. Besides, a new strong band at 1701 cm^{-1} is found in the spectrum of the cross-linked PS membranes, and can be assigned to C=O groups, as reported by Dai *et al.* ,[40] the oxidation product of FDA residual segments by the catalyst of Fe (III).[40, 43] The structure of the cross-linked PS membrane was further confirmed by the Solid-state NMR. In Fig 4, solid-state ^{13}C cross-polarization magic angle spinning NMR spectroscopy shows resonance peaks near 138 and 128 ppm, which are belonged to aromatic carbon and non-substituted aromatic carbon, respectively. The resonance peak near 40 ppm can be assigned to the carbon in the methylene linker forming in the cross-linking reaction. These results are completely consistent with the data reported by Tan *et al.*[47] Besides, the resonance peaks between 150 and 200 ppm indicate the formation of the C=O group ; this phenomenon is consistent with the observation reported by Dai *et al.*, as well as the results of the FT-IR spectra.[40] All the above spectra data confirm that the PS

membranes have reacted with FDA, and the hyper-cross-linked structure formed.

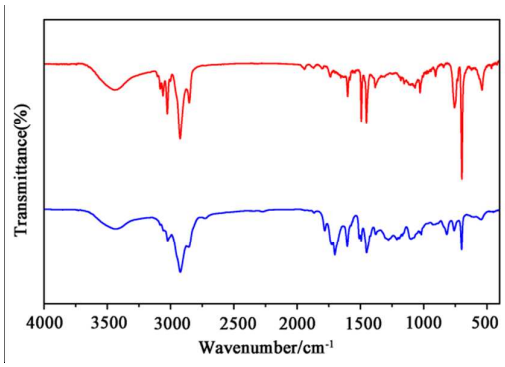

Fig 3 FT-IR spectra of the PS membrane before (red curve) and after (blue curve) hyper-cross-linking reaction

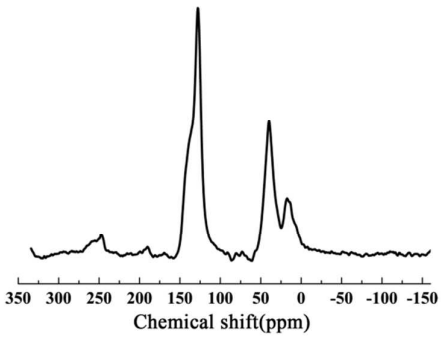

Fig 4 Solid-state NMR spectrum of the hyper-cross-linked PS membrane.

The membranes after hyper-cross-linking reaction were observed by SEM and TEM. From the morphology of cross-linked PS membrane shown in Fig 5a, we can find that although PS is soluble in DCE, the porous structure features by the CXL processed membranes is well preserved after the hyper-cross-linking reaction (The histogram of macro pore sizes distribution after hyper-cross-linking process calculated according to the SEM image is shown in Figure S1 b). The reason is that the hyper-cross-linking reaction is very rapid,[40] and the cross-linked layer formed quickly on the membrane surface, preventing further deformation and dissolution of the membrane. Slight deformation of the pores is observed, due to the plasticization effect of DCE on PS matrix. Dai *et al*. have confirmed that a membrane with the thickness of 50 μm is completely cross-linked after 6 h reaction, owing to the faster mass transport in the PS membrane.[41] Therefore, it is safe to conclude that the micropores are distributed throughout the entire membranes after 8 h hyper-cross-linking reaction. The structure generated during hyper-cross-linking reaction was observed by TEM, as shown in Fig 5b. Obviously, small pores were found throughout the sample, confirming that micropores were generated during the hyper-cross-linking reaction.

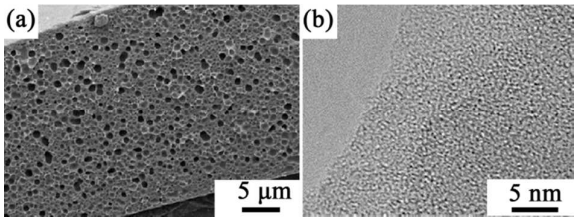

Fig 5 (a) Cross-sectional SEM image and (b) TEM image of the hyper-cross-linked PS membrane.

We further use N_2 adsorption technique to investigate the surface area and pore size of the cross-linked PS membrane.[48] The N_2 adsorption-desorption isotherms of the membranes (Fig 6a-black curve) exhibit a Type I reversible sorption profile with a slight hysteresis loop at higher relative pressures, indicating the presence of abundant micropore structure accompanied with a few mesopores in the membrane. According to the isotherms, the BET surface area of the membrane is calculated to be 270.8 $m^2\ g^{-1}$. Such a high specific surface area indicates that the micropores in the membrane are interconnected and accessible to gas molecules. The pore size distribution calculated using the Barrett–Joyner–Halenda (BJH) method is shown in Fig 6b. The membrane shows a dominant pore size of 0.87 ~ 2.0 nm, in good agreement with the results of TEM image. Also a small number of mesopores are observed in Fig 6b. The results of N_2 adsorption analysis further confirm the microporous structures in the cross-linked PS membrane. In summary, the above electron microscopic images reveal that the cross-linked PS membranes are hierarchically porous materials, with macropores formed in CXL process, and micropores of 1 ~ 2 nanometers generated by the hyper-cross-linking reaction.

The cross-linking reaction not only generate micropores in the membrane, but also increase the thermal stability of the membrane. The N_2 adsorption/desorption curves of the cross-linked PS membrane after heated at 150 °C for 0.5 h are shown in Fig 6a (red line), and the specific surface area is calculated to be 244.5 $m^2\ g^{-1}$. Thus the surface area change hardly after thermal treatment, indicating that the micropore structures are well preserved after thermal treatment. Noticing that the glass transition point of PS is 100 °C, the above results clearly demonstrate that the thermal stability of the PS membrane is significantly improved by the cross-linking structure. The cross-linking reaction also increase the decomposition temperature of the PS membrane, as shown in the TGA curves (Fig S1). The residual weight of hyper-cross-linked PS membrane at 550 °C is 32.9%, while that of the uncross-linked membrane is only 1.29%.

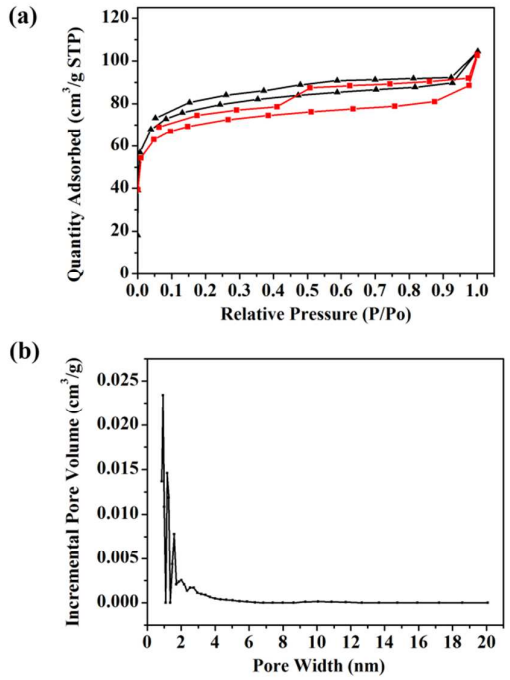

Fig 6 (a) N_2 adsorption/desorption curves of the cross-linked PS membrane before (black) and after (red) heating at 150 °C for 0.5 h. (b) Pore size distribution of the hierarchically porous PS membrane.

Conclusions

In conclusion, we prepared hierarchically porous polymeric films with a commercially available polymer. The first level of macro-scale structures was produced by selectively swelling the surfactant micelles embedded in the polymer matrix with a CXL treatment, while the second level of micropores was created *via* the sequent hyper-cross-linking reaction. The hierarchical porosity is confirmed by SEM, TEM and BET measurements. It is should be noted that the hyper-cross-linking reaction not only creates the specific surface area, but also improves the thermal stability of the hierarchical porosity. This method is not only suitable for PS and PS-based copolymers, but also applicable to many other polymers which bear aromatic rings and are active in Friedel-Crafts reactions.[26] Since PS can also be cross-linked by UV irradiation,[49, 50] therefore, photochemical reaction is the alternative strategy for the formation of hyper-cross-linking structures, which is currently under investigation. Moreover, other types of surfactants, such as amphiphilic block copolymers, can also be used in our method, and are expected to generate different pore structures and further functionalization. We believe that the etching-free and versatile mythology will demonstrate its promising applications in catalysis, separation and gas storage.

Acknowledgements

L. L. gratefully acknowledges the National Natural Science Foundation of China (No. 51373143 and 21174116), the Natural Science Foundation of Fujian Province (No. 2014J0105), the fund of State Key Lab for Modification of Chemical Fibers and Polymer Materials and the Fundamental Research Funds for the Central Universities (No. 2013SH003).

Notes and references

1 T. Nishikawa, J. Nishida, R. Ookura, S. I. NiShimura, S. Wada, T. Karino and M. Shimomura, *Mater. Sci. Eng., C*, 1999, **8-9**, 495-500.
2 D. L. Gin and R. D. Noble, *Science*, 2011, **332**, 674-676.
3 R. M. Dorin, H. Sai and U. Wiesner, *Chem. Mater.*, 2014, **26**, 339-347.
4 Y. Li, Z. Y. Fu and B. L. Su, *Adv. Funct. Mater.*, 2012, **22**, 4634-4667.
5 X. Y. Yang, A. Léonard, A. Lemaire, G. Tian and B. L. Su, *Chem. Commun.*, 2011, **47**, 2763-2786.
6 S. Valkama, A. Nykänen, H. Kosonen, R. Ramani, F. Tuomisto, P. Engelhardt, G. ten Brinke, O. Ikkala and J. Ruokolainen, *Adv. Funct. Mater.*, 2007, **17**, 183-190.
7 D. Lee, C. Zhang, C. Y. Wei, B. L. Ashfeld and H. F. Gao, *J. Mater. Chem. A*, 2013, **1**, 14862-14867.
8 H. Sai, K. W. Tan, K. Hur, E. Asenath-Smith, R. Hovden, Y. Jiang, M. Riccio, D. A. Muller, V. Elser, L. A. Estroff, S. M. Gruner and U. Wiesner, *Science*, 2013, **341**, 530-534.
9 M. G. Schwab, I. Senkovska, M. Rose, N. Klein, M. Koch, J. Pahnke, G. Jonschker, B. Schmitz, M. Hirscher and S. Kaskel, *Soft Matter*, 2009, **5**, 1055-1059.
10 L. L. C. Wong, P. M. B. Villafranca, A. Menner and A. Bismarck, *Langmuir*, 2013, **29**, 5952-5961.
11 J. Gao, J. S. P. Wong, M. J. Hu, W. Li and R. K. Y. Li, *Nanoscale*, 2014, **6**, 1056-1063.
12 C. Park, J. Yoon and E. L. Thomas, *Polymer*, 2003, **44**, 6725-6760.
13 Z. S. Ge and S. Y. Liu, *Macromol. Rapid Commun.*, 2009, **30**, 1523-1532.
14 B. D. Olsen and R. A. Segalman, *Mater. Sci. Eng., R*, 2008, **62**, 37-66.
15 F. S. Bates and G. H. Fredrickson, *Phys. Today*, 1999, **52**, 32-38.
16 J. T. Chen, E. L. Thomas, C. G. Zimba and J. F. Rabolt, *Macromolecules*, 1995, **28**, 5811-5818.
17 Z. S. Ge and S. Y. Liu, *Chem. Soc. Rev.*, 2013, **42**, 7289-7325.
18 A. Horechyy, B. Nandan, N. E. Zafeiropoulos, P. Formanek, U. Oertel, N. C. Bigall, A. Eychmueller and M. Stamm, *Adv. Funct. Mater.*, 2013, **23**, 483-490.
19 R. Takekoh and T. P. Russell, *Adv. Funct. Mater.*, 2014, **24**, 1483-1489.
20 T. Jin, Z. C. Xiong, X. Zhu, N. Mehio, Y. J. Chen, J. Hu, W. B. Zhang, H. F. Zou, H. L. Lai and S. Dai, *ACS Macro Lett.*, 2015, **4**, 570-574.
21 K. W. Tan, B. Jung, J. G. Werner, E. R. Rhoades, M. O. Thompson and U. Wiesner, *Science*, 2015, **349**, 54-58.
22 J. L. Gong, A. J. Zhang, H. Bai, Q. K. Zhang, C. Du, L. Li, Y. Z. Hong and J. Li, *Nanoscale*, 2013, **5**, 1195-1204.
23 A. J. Zhang, Q. K. Zhang, H. Bai, L. Li and J. Li, *Chem. Soc. Rev.*, 2014, **43**, 6938-6953.
24 P. G. Jessop and B. Subramaniam, *Chem. Rev.*, 2007, **107**, 2666-2694.
25 R. Zhang and H. Yokoyama, *Macromolecules*, 2009, **42**, 3559-3564.
26 S. J. Xu, Y. L. Luo and B. E. Tan, *Macromol. Rapid Commun.*, 2013, **34**, 471-484.
27 N. Fontanals, M. Galià, P. A. G. Cormack, R. M. Marcé, D. C. Sherrington and F. Borrull, *J. Chromatogr. A*, 2005, **1075**, 51-56.

28 Y. Sun, J. L. Chen, A. M. Li, F. Q. Liu and Q. X. Zhang, *React. Funct. Polym.*, 2005, **64**, 63-73.
29 J. Germain, J. M. J. Frechet and F. Svec, *J. Mater. Chem.*, 2007, **17**, 4989-4997.
30 Y. H. Zhang, Y. D. Li, F. Wang, Y. Zhao, C. Zhang, X. Y. Wang and J. X. Jiang, *Polymer*, 2014, **55**, 5746-5750.
31 M. P. Tsyurupa and V. A. Davankov, *React. Funct. Polym.*, 2002, **53**, 193-203.
32 B. C. Pan, Y. Xiong, A. M. Li, J. L. Chen, Q. X. Zhang and X. Y. Jin, *React. Funct. Polym.*, 2002, **53**, 63-72.
33 S. Wang and M. L. Robertson, *ACS Appl. Mater. Interfaces*, 2015, **7**, 12109−12118.
34 S. Siripurapu, J. A. Coughlan, R. J. Spontak and S. A. Khan, *Macromolecules*, 2004, **37**, 9872-9879.
35 K. Senshu, S. Yamashita, H. Mori, M. Ito, A. Hirao and S. Nakahama, *Langmuir*, 1999, **15**, 1754–1762.
36 K. Senshu, S. Yamashita, M. Ito, A. Hirao and S. Nakahama, *Langmuir*, 1995, **11**, 2293–2300.
37 M. W. Matsen and F. S. Bates, *Macromolecules*, 1996, **29**, 1091-1098.
38 L. Li, T. Nemoto, K. Sugiyama and H. Yokoyama, *Macromolecules*, 2006, **39**, 4746-4755.
39 H. Yokoyama and K. Sugiyama, *Macromolecules*, 2005, **38**, 10516-10522.
40 Z. A. Qiao, S. H. Chai, K. Nelson, Z. G. Bi, J. H. Chen, S. M. Mahurin, X. Zhu and S. Dai, *Nat. Commun.*, 2014, **5**, 3705.
41 Q. Q. Liu, L. Wang, A. G. Xiao, H. J. Yu and Q. H. Tan, *Eur. Polym. J.*, 2008, **44**, 2516-2522.
42 G. Q. Xiao, R. M. Wen, D. M. Wei and D. Wu, *J. Hazard. Mater.*, 2014, **280**, 97-103.
43 R. V. Law, D. C. Sherrington, C. E. Snape, I. Ando and H. Kurosu, *Macromolecules*, 1996, **29**, 6284-6293.
44 G. Q. Xiao, L. C. Fu and A. M. Li, *Chem. Eng. J.*, 2012, **191**, 171-176.
45 B. Y. Li, X. Huang, L. Y. Liang and B. E. Tan, *J. Mater. Chem.*, 2010, **20**, 7444-7450.
46 B. Y. Li, F. B. Su, H. K. Luo, L. Y. Liang and B. E. Tan, *Microporous Mesoporous Mater.*, 2011, **138**, 207-214.
47 B. Y. Li, R. N. Gong, W. Wang, X. Huang, W. Zhang, H. M. Li, C. X. Hu and B. E. Tan, *Macromolecules*, 2011, **44**, 2410-2414.
48 S. J. Gregg and K. S. W. Sing, *Adsorption, Surface Area and Porosity,* Academic Press, London, UK, 1982.
49 L. Li, Y. W. Zhong, J. Li, C. K. Chen, A. J. Zhang, J. Xu and M. Zhi, *J. Mater. Chem.*, 2009, **19**, 7222-1227.
50 L. Li, Y. W. Zhong, C. Y. Ma, J. Li, C. K. Chen, A. J. Zhang, D. L. Tang, S. Y. Xie and M. Zhi, *Chem. Mater.*, 2009, **21**, 4977-4983.